Both sunitinib and sorafenib are effective treatments for pheochromocytoma in a xenograft model

M. Denorme, Laurent Yon, Clément Roux, B.J. J Gonzalez, Emmanuel
Baudin, Y. Anouar, C. Dubessy

Both sunitinib and sorafenib are effective treatments for pheochromocytoma in a xenograft model

M. Denorme [a,b,c], L. Yon [a,b,c], C. Roux [b,d,e], B.J. Gonzalez [b,d,e], E. Baudin [f], Y. Anouar [a,b,c,*,1], C. Dubessy [a,b,c,1]

[a] Institut National de la Santé et de la Recherche Médicale (INSERM), U982, Mont-Saint-Aignan, France
[b] Normandie Univ, Caen, France
[c] University of Rouen, Laboratory of Neuronal and Neuroendocrine Differentiation and Communication, Institute for Research and Innovation in Biomedicine (IRIB), Mont-Saint-Aignan, France
[d] Haute-Normandie-INSERM ERI28, Rouen, France
[e] University of Rouen, Laboratory of Microvascular Endothelium and Neonate Brain Lesion, Institute for Research and Innovation in Biomedicine, Rouen, France
[f] Departments of Nuclear Medicine and Endocrine Tumors, Institut Gustave-Roussy, Villejuif, France

Introduction

Pheochromocytomas (PCC) are rare neuroendocrine tumors that arise from chromaffin cells of the adrenal medulla or extra-adrenal sites (referred to as paragangliomas). These tumors are characterized by an excess of catecholamine release, leading mainly to hypertension [1]. The other symptoms are variable and nonspecific, including headaches, palpitations, diaphoresis, weight loss and diabetes. The majority of PCC are sporadic, but there is even so 30–35% that are associated with an hereditary syndrome due to a germline mutation in one of several susceptibility genes identified to date, including the RET proto-oncogene, the tumor suppressor genes neurofibromin 1 and von Hippel–Lindau (VHL), the subunits of the succinate dehydrogenase (SDHx) enzyme SDHA, B, C, D, and SDHAF2, and the recently discovered TMEM127, MAX and fumarate hydratase [2,3]. Commonly, PCC subtypes can be divided in two clusters based on their gene expression profile. The first cluster of PCC is characterized by mutations in SDHx and VHL genes leading to dysregulation of hypoxia inducible factor-associated pathways and increased angiogenesis [4], while the second cluster is characterized by RET, neurofibromin 1 or TMEM127 mutations which are associated with activation of PI3K/AKT/mTORC and RAS/RAF/ERK pathways [5].

* Corresponding author at: INSERM U982, Lab. Neuronal and Neuroendocrine Differenciation and Communication, University of Rouen, 76821 Mont-Saint-Aignan, France. Tel.: +33 235 14 66 61; fax: +33 235 14 69 46.
E-mail address: youssef.anouar@univ-rouen.fr (Y. Anouar).
[1] Y.A. and C.D. should be considered as co-last authors.

While benign tumors are usually resected surgically with a high survival rate for patients, there is no curative treatment for most patients with metastatic PCC. This lack of effective therapy leads to a 5-year mortality rate of 50–60% [6]. Malignancy occurs in about 15–17% of PCC cases, but higher proportions have also been reported depending on the location of the primary tumor and the underlying germline mutation [7,8]. Nowadays there is still no reliable criterion to diagnose malignancy, except the presence of metastases in lymph nodes, bones, lungs and liver. Among the proposed malignancy indicators, overexpression of vascular endothelial growth factor (VEGF) has been reported [9–11]. VEGF is a pro-angiogenic factor notably secreted by tumor cells, which stimulates the proliferation and migration of endothelial cells resulting in the outgrowth of new capillaries into the tumor. Therefore, the VEGF signaling pathway is essential to neo-angiogenesis which corresponds to the growth of new blood vessels from preexisting vessels. It has been shown that malignant PCC together with SDHx and VHL-related PCC are very highly vascularized tumors with abnormal vascular architecture that is associated with a strong angiogenesis [12–14].

Angiogenesis is a rate-limiting process in tumor growth and malignancy. Targeting neo-vascularization as a therapeutic strategy has led to the development of small specific inhibitors such as sunitinib and sorafenib. These compounds which are receptor tyrosine kinase (RTKs) inhibitors targeting the VEGF signaling pathway [15], have already been evaluated in several clinical trials. Sunitinib inhibits numerous RTKs including VEGFRs, PDGFR, Flt-3, c-kit, CSF-1R, and RET, and has been approved by the Food and Drug Administration (FDA) for the treatment of advanced renal cell carcinoma and gastro-intestinal stromal tumors. Sorafenib inhibits VEGFR-2 and -3, PDGFR-B, Flt-3 and c-kit as well as the raf protein kinase. Sorafenib has also been approved by FDA for the treatment of renal cell carcinoma and hepatocellular carcinoma.

Given the hypervascularization and the significant angiogenesis found in malignant PCC and other PCC subtypes, targeted anti-angiogenic therapies have recently been proposed for the treatment of this tumor. Indeed, case reports [16–20] and a clinical study [21] have shown promising results after administration of sunitinib to patients with malignant paraganglioma or PCC. However, these assays only tested sunitinib and have been conducted for some of them on a limited number of patients. In this context, the aim of our study was to provide further pre-clinical evidence for the use of anti-angiogenic treatments for PCC. To achieve this goal, we investigated the action of sunitinib and sorafenib using a PCC cell line and a xenograft mouse model. The effects of both drugs were tested and compared *in vivo* on tumor growth and neo-angiogenesis, and *in vitro* on PCC cell survival.

Materials and methods

Materials

Sunitinib and sorafenib were purchased from LC Laboratories (Woburn, USA). For *in vitro* studies, they were dissolved in dimethyl sulfoxide (DMSO) at a concentration of 10 mM and then diluted to appropriate final concentrations in Dulbecco's modified Eagle Medium (DMEM, Invitrogen, Cergy Pontoise, France). DMSO did not exceed 0.3% in the final solution. For *in vivo* testing, sunitinib and sorafenib were prepared at a final concentration of 8 mg/mL. Sunitinib was diluted in Ora+/water (1/1, v/v; Paddock Laboratories, Colombes, France) and sorafenib in CremophorEL/ethanol (1/1, v/v; Sigma–Aldrich, St-Quentin-Fallavier, France) and then diluted in water (1/4, v/v).

PC12 cell culture

The rat pheochromocytoma-derived, undifferenciated PC12 cells were purchased from the European Collection of Cell Culture (Salisbury, Wilshire, UK) and cultured in DMEM supplemented with 10% horse serum, 5% fetal bovine serum, 1% L-glutamine and 1% penicillin–streptomycin in 5% CO_2/95% O_2 humidified atmosphere at 37 °C. Unless otherwise indicated, cell culture reagents were obtained from Sigma–Aldrich.

Cell viability

PC12 cells were plated at a density of 5×10^3 cells per well in 96-well plate and incubated overnight. On the following day, compounds were added to the wells and incubated for an additional 2–72 h. Cells were cultured in triplicate for each condition and experiments were reproduced 3 times. Cell viability was measured after 72 h using the CellTiter-Blue Cell Viability Assay kit (Promega, Charbonnière, France) according to the manufacturer's instructions. The IC_{50} value (half maximal inhibitory concentration) was calculated from dose–response curves by nonlinear regression analysis. Apoptosis was measured from 2 to 24 h using Apo-ONE® Homogeneous Caspase-3/7 Assay (Promega). Luminescence and fluorescence measurements were performed using the microplate reader FlexStation3 (Molecular Devices, Saint-Grégoire, France).

Animals

Seven week-old male athymic Swiss nude mice *nu/nu* (Charles River Laboratory, l'Arbresle, France) were used for *in vivo* studies. They were housed and maintained under standard laboratory conditions (21 °C, 12:12 h light–dark cycle) and received food and water *ad libitum*. Experiments were conducted in accordance with the regional ethics committee on animal experimentation and in compliance with the EC animal welfare regulations.

Mouse xenograft model

Prior to implantation, PC12 cells were harvested during exponential growth by trypsinization and were then washed thoroughly. Mice received a subcutaneous injection of 5×10^5 cells in a volume of 100 μL into the hind flank at day 0 (D0). During the next 14 days, implanted cells grew to form a tumor. When the tumor became measurable (3–4 mm³, around D14), animals were then randomized into control or treated (sunitinib or sorafenib) groups of 10 mice each. Treated mice were daily force-fed with 5 μL/g (40 mg/kg) of sunitinib or sorafenib during a period of 14 days (D15–D28). This dose was used in several other studies in mice and was chosen because it yields plasma concentrations comparable to those found in patients treated with these drugs [22–24]. Control animals received the vehicle.

Tumor dimensions, assessed using Vernier calipers, and mice body weight were measured three times a week. The tumor volume was calculated using the formula $V = width^2 \times length \times 0.52$. The relative tumor volume (RTV) was calculated by dividing the tumor volume at any time by the tumor volume at the beginning of the treatment. Tumor growth curves were obtained by plotting the mean RTV against time for each experimental group. The tumor doubling time (TDT) and the tumor growth delay (TGD) were determined using the growth curve part corresponding to the treatment period. TDT was calculated using the equation $TDT = (T - T_0) \times log2/logV - logV_0$ (where $T - T_0$ indicates the duration between two measurements and V and V_0 denotes the tumor volume at two points of measurement). TGD was calculated as the time, expressed as days, required for tumors to reach a x-fold increase (between 3 and 5) in relative tumor volume.

After the treatment period (D28), half of each mice group was euthanized, tumors were excised, frozen at −25 °C in isopentane and stored at −80 °C until use. The other mice were maintained alive one more week (D35) for tumor growth measurement after treatment withdrawal, and then euthanized.

Immunohistochemistry

Angiogenesis and apoptosis were investigated by immunohistochemistry. The vascular network was immunolabeled using a rabbit polyclonal CD31 antibody that recognizes endothelial cells (Abcam, Paris, France, diluted 1:300). A cleaved caspase-3 rabbit antibody (Cell Signaling Technology, Saint Quentin Yvelines, France, diluted 1:500) was used to identify apoptotic cells. Frozen tumors were 8–10 μm-thick sectioned (Cryostat cryomicrocut 3050, Leica, Solms, Germany), mounted on superfrost slides (Menzel-Glaser, Braunschweig, Germany) and air-dried for 2 h. Sections were fixed in 4% paraformaldehyde for 20 min, washed twice in phosphate buffered saline (PBS, pH 7.4), incubated for 1 h at room temperature in a blocking buffer and then overnight at 4 °C with one of the two different primary antibodies. The slides were then washed in PBS and incubated with goat anti-rabbit (GAR)/Alexa-488 secondary antibody for 2 h at room temperature. After several rinses in PBS and incubation with the nuclear dye 4,6-diamino-2-phenylindole (DAPI) for 1 min, sections were coverslipped with Fluoroshield mounting medium (Sigma–Aldrich).

Image analysis

Image acquisitions were performed with a conventional microscope (Nikon, Champigny-sur-Marne, France). At least 5 animals per group and 2 distant slices per tumor were examined for the quantification of the intratumoral vascularization.

Five fields were randomly chosen at 20× magnification excluding the necrotic zone, and stored as TIFF files. In order to obtain objective measurements of the vessels architecture, an automated script was developed using various plug-ins added to Fiji open-source software [25]. Automatically, the macrodetected the labeled tubular structures on acquired images. A stained tube with two end-points was considered as a microvessel. The images were then thresholded to fit with the vascular morphology and to reduce background noise, and the microvascular area was calculated. The thresholded images were then skeletonized to obtain the number and the length of branches, and the number of nodes per microvessel. The data were plotted against treatments.

In order to measure apoptosis, 8 μm-thick tumor slices were scanned using the Nanozoomer 2.0 HT scanner (Hamamatsu, Massy, France) to get a global view of the caspase-3 labeling. The images were then examined with Fiji software, thresholded and binarized to quantify the global apoptotic staining normalized to the tumor slice area.

Statistical analysis

Data were plotted and analyzed using the Prism 4 program (GraphPad Software, Inc., San Diego, CA, USA). Non-parametric tests were used to compare the relative tumor volume, tumor weight, caspase-3 labeling (Kruskal–Wallis) and the vascular architecture parameters (Two-Way ANOVA) between controls and treated animals. Probability values <0.05 were considered significant.

Results

Sunitinib and sorafenib inhibit the growth of pheochromocytoma cell xenografts

Oral administration of sunitinib or sorafenib (40 mg/kg/day) for 14 days provoked a significant inhibition of tumor growth in treated compared to control animals (from D28 and D25 until the end of the experiment, respectively, Fig. 1A and B). Tumors from treated animals exhibited a significantly higher TDT than those of the control groups (10.6 days for sunitinib, 7.4 days for sorafenib vs. 5.5 days for controls; $P < 0.05$). The TGD were 7 and 8 days for sunitinib and sorafenib treatments, respectively. At the end of the experiment, tumor volume was reduced by 60% after sunitinib treatment (722 ± 175 mm^3 vs. 1765 ± 378 mm^3 at D35, $P < 0.001$) and by 71% for sorafenib (478 ± 83 mm^3 vs. 1654 ± 382 mm^3 at D34, $P < 0.001$). As shown in Fig. 1C and D, the inhibition of tumor growth led to a significant tumor weight loss of 70% and 73% after sunitinib (D35) and sorafenib (D34) treatments, respectively ($P < 0.05$).

Sunitinib and sorafenib inhibit tumor neo-angiogenesis in pheochromocytoma cell xenografts

Macroscopic examination of control tumors at D28 and D34–35 (Fig. 2A and D) showed the occurrence of numerous and thick peritumoral vessels. In contrast, tumors in animals treated with sunitinib (Fig. 2B) or sorafenib (Fig. 2C) were much less surrounded by these vessels than controls. At the end of the experiment, 7 days after the treatment period (D34–35), the number of vessels irrigating the tumors increased again in the previously treated tumors (Fig. 2E and F).

Tumoral neo-angiogenesis was assessed by morphometric analysis of the vascular network after CD31 immunolabeling (Fig. 3). As illustrated in Fig. 3A and D, subcutaneous injection of PC12 cells led to the growth of tumors strongly invaded by microvessels. Control tumors showed a rich vascularization, with a dense network of long and tortuous microvessels (Fig. 3A and D). These vessels displayed linked segments of irregular length, frequently exhibiting 2 or 3 branchings. These tight vascular structures seem to delineate nodules of tumor tissue. In contrast, Fig. 3B and C show that tumors from treated mice display only a weak vascular network represented by few scattered labeled endothelial cells. However,

one week after the treatment period, tumors exhibited again numerous and long vessels (Fig. 3E and F).

Quantitative analysis showed that the microvascular area is drastically reduced by 85% and 80% following sunitinib and sorafenib treatment at D28, respectively (Fig. 4A; $P < 0.01$ and $P < 0.001$, respectively). Both treatments also significantly diminished the number of nodes per field (−84% for sunitinib and −73% for sorafenib; Fig. 4B; $P < 0.001$) and the number of branches per field (−84% for sunitinib and −87% for sorafenib; Fig. 4C; $P < 0.001$). Both compounds showed a strong inhibition of the mean vessel length (−80% for sunitinib and −78% for sorafenib; Fig. 4D; $P < 0.01$ and $P < 0.001$, respectively). The treatments inhibited the sprouting and the growth of microvessels, as illustrated by Fig. 4E and F which show that sunitinib and sorafenib reduced significantly the number of nodes (−95% and −84%; $P < 0.01$ and $P < 0.05$, respectively) and branches (−30% and −27%; $P < 0.01$ and $P < 0.05$, respectively) per microvessel. At the end of the assay, one week after treatment completion (D34–35), all the six parameters analyzed in tumor slices from treated animals were significantly increased compared to D28 values. However, except for the number of branches and nodes per microvessel (Fig. 4E and F), the different parameters including the microvascular area or the length of branches remained significantly reduced compared to control values at D34–35 (Fig. 4A–D).

Sunitinib and sorafenib induce apoptosis in pheochromocytoma cell xenografts

Staining of cleaved caspase-3-positive cells revealed distinct profiles: control tumors were characterized by few and isolated apoptotic cells (Fig. 5A), whereas sunitinib- and sorafenib-treated tumors displayed numerous grouped apoptotic cells (Fig. 5B and C). Indeed, the quantification revealed a significant increase in the surface of apoptotic zones after sunitinib and sorafenib treatment (5.6-fold and 3.5-fold; Fig. 5G; $P < 0.01$ and $P < 0.001$, respectively). Of note, treatment interruption caused a dramatic decrease in apoptotic levels for both drugs (Fig. 5D–F), which were comparable to those of controls (Fig. 5G).

Sunitinib and sorafenib decrease the viability of PC12 cells

In order to evaluate if sunitinib and sorafenib could have a direct effect on pheochromocytes, cultured PC12 cells were exposed to increasing concentrations of these compounds, and cell viability was assessed after 72 h exposure (Fig. 6). Sunitinib and sorafenib inhibited PC12 cell viability following biphasic curves, likely reflecting inhibition of proliferation and cytotoxicity. Thus, sunitinib exerted an anti-proliferative effect of 30% at the nanomolar range ($LogIC50_1 = -7.15 \pm 0.23$; 0.07 μM) and a cytotoxic effect at the micromolar range ($LogIC50_2 = -5.36 \pm 0.05$; 4.35 μM) (Fig. 6A). Similarly, low doses of sorafenib exerted a 55% inhibition of cell proliferation ($LogIC50_1 = -7.77 \pm 0.24$; 0.02 μM), whereas high doses provoked cytotoxic effects ($LogIC50_2 = -4.33 \pm 0.13$; 46.7 μM) (Fig. 6B).

Sunitinib exerts a pro-apoptotic effect in PC12 cells

Analysis of PC12 cell apoptosis revealed an effect of sunitinib at a dose of 30 μM as early as 4 h after the onset of the treatment (Fig. 6C). Of note, the apoptotic level at 24 h is low because the majority of the cells already died at this time point (data not shown). In contrast, whatever the dose and incubation period, sorafenib had no apoptotic effect (Fig. 6D).
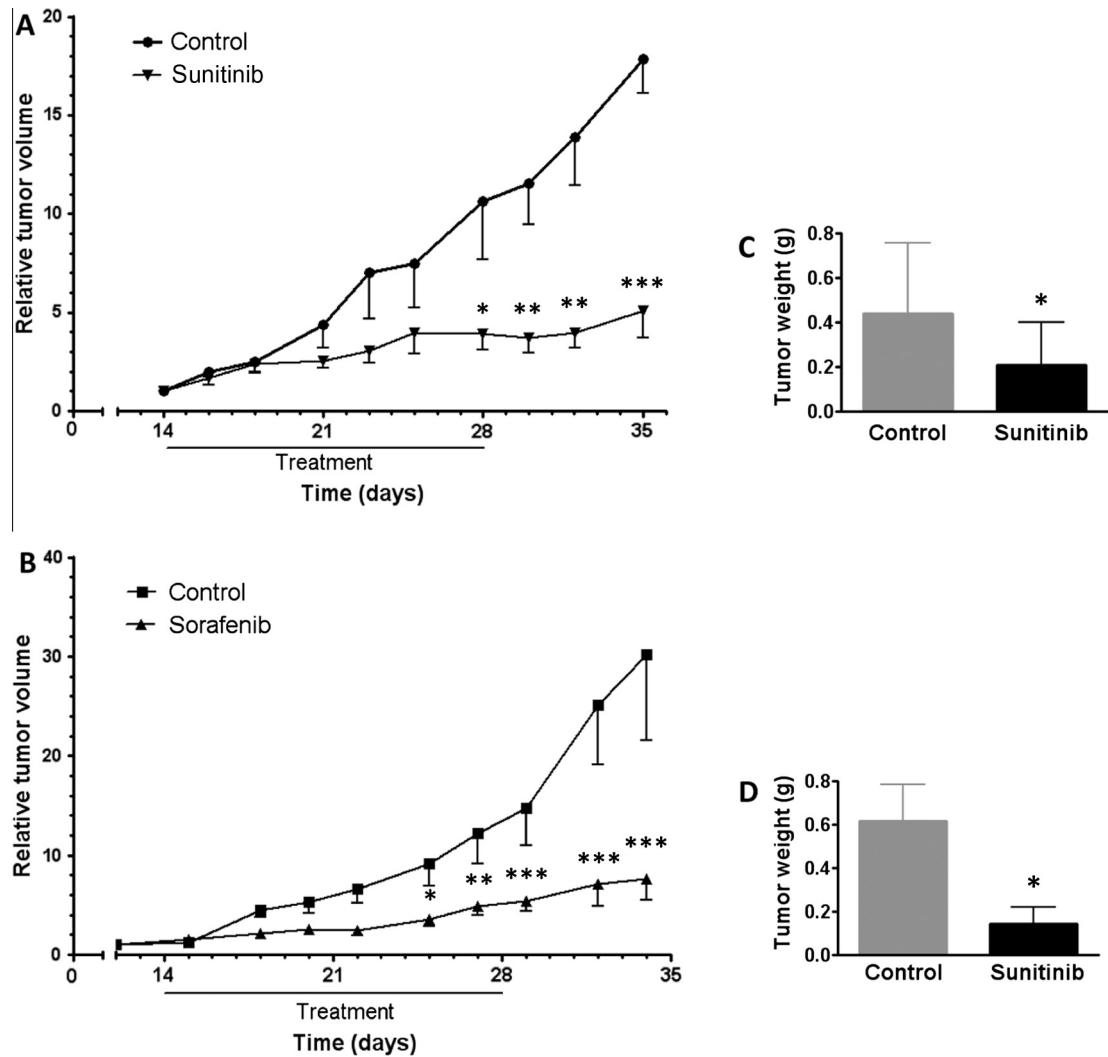
Fig. 1. Effect of sunitinib and sorafenib on PC12 cell xenograft in nude mice. PC12 cells (5×10^5) were implanted subcutaneously and left during 14 days (D0–D14) to form a tumor. Animals were then treated daily with sunitinib or sorafenib for 14 days (D14–D28). Control animals received the excipient (Ora+ or CremophorEL, respectively). From D28 or D25 to D34/35, respectively for sunitinib and sorafenib treatment, a significant decrease in RTV was observed in comparison to control groups (A and B). Tumor weight was significantly decreased by sunitinib (−70% at D35, $P < 0.05$, C) and sorafenib (−73% at D34, $P < 0.05$, D). For data expressed as RTV, each tumor volume is normalized to D14. ●, Ora+ control animals; ■, CremophorEL control animals; ▼, sunitinib-treated mice; ▲, sorafenib-treated mice. $^*P < 0.05$, $^{**}P < 0.01$ and $^{***}P < 0.001$.

Discussion

Currently, no curative treatment options are available for malignant PCC. An important feature of these malignant tumors and all VHL and SDHx-associated tumors in general is their hypervascularization, which suggests that anti-angiogenic drugs could represent efficient treatments [12,26–28]. Recently, a clinical study and case reports of oral administration of sunitinib showed promising results in patients with PCC or paraganglioma [21,29,30]. In particular, Ayala-Ramirez et al. reported several benefits of sunitinib in some patients with progressive metastatic pheochromocytoma in terms of tumor size reduction and disease stabilization [21]. Moreover, the approval of sunitinib use for pancreatic neuroendocrine tumors [31] also supports the idea that anti-angiogenic therapy could be effective in other neuroendocrine neoplasms. Due to its ability to directly inhibit the raf protein kinase in addition to RTKs, sorafenib also represents an interesting therapeutic tool. In fact, this anti-angiogenic drug has never been evaluated for PCC treatment. Therefore, in the present study, we investigated and compared for the first time the effect of sunitinib and sorafenib in a xenograft model of PCC. We demonstrated that after two weeks of oral administration in mice, both drugs were highly effective

on PC12 cell xenograft tumors, with a drastic reduction of tumor growth and volume, accompanied by impaired angiogenesis.

Since no suitable human PCC cell line was available, we used the rat PC12 cell line to generate a model system of PCC in a xenograft. Injection of PC12 cells in nude mice led to tumor development with a comparable growth curve to that previously described using a similar xenograft model [32]. Treatment with sunitinib or sorafenib strongly slowed down tumor growth with no difference in potency and efficacy. Using a different administration mode (intravenous), Maitani et al. described a similar efficacy of sunitinib in another PC12 cell xenograft model [33]. Interestingly, the extent of tumor volume inhibition observed in our study was similar to that reported for sunitinib and sorafenib, used at comparable doses, in a xenograft model of human renal cell carcinoma [24].

Endothelial staining showed a very dense, irregular and tortuous vascular architecture in PC12 cell xenograft slices, which is reminiscent of the hypervascularization observed in malignant pheochromocytoma [9]. After two weeks of treatment with each compound, we found a significant and dramatic decrease in the parameters characterizing tumoral neo-angiogenesis, i.e. microvascular area, length and number of branches, and the number of
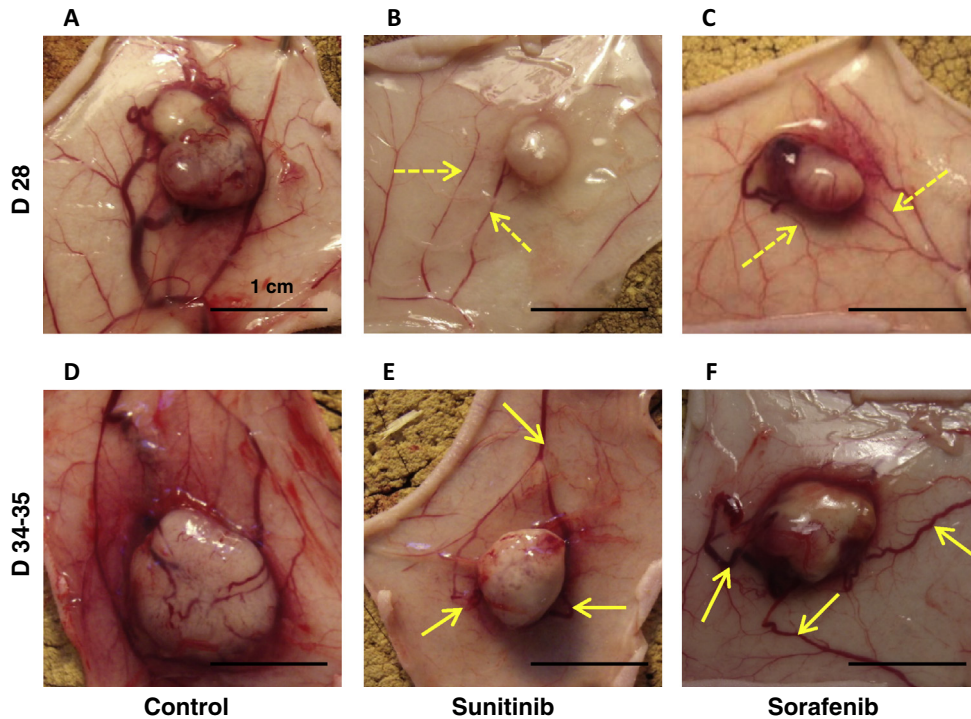
Fig. 2. Representative photographs of formed tumors excised from control and sunitinib- or sorafenib-treated mice. At the end of drug administration (D28), treated tumors (B and C) were smaller, paler and less irrigated by peripheral vessels (dotted arrows) than controls (A). One week after treatment withdrawal (D34/35), tumors (E and F) were still smaller and less irrigated than controls (D) but thicker vessels were observed (arrows). Scale bar, 1 cm.
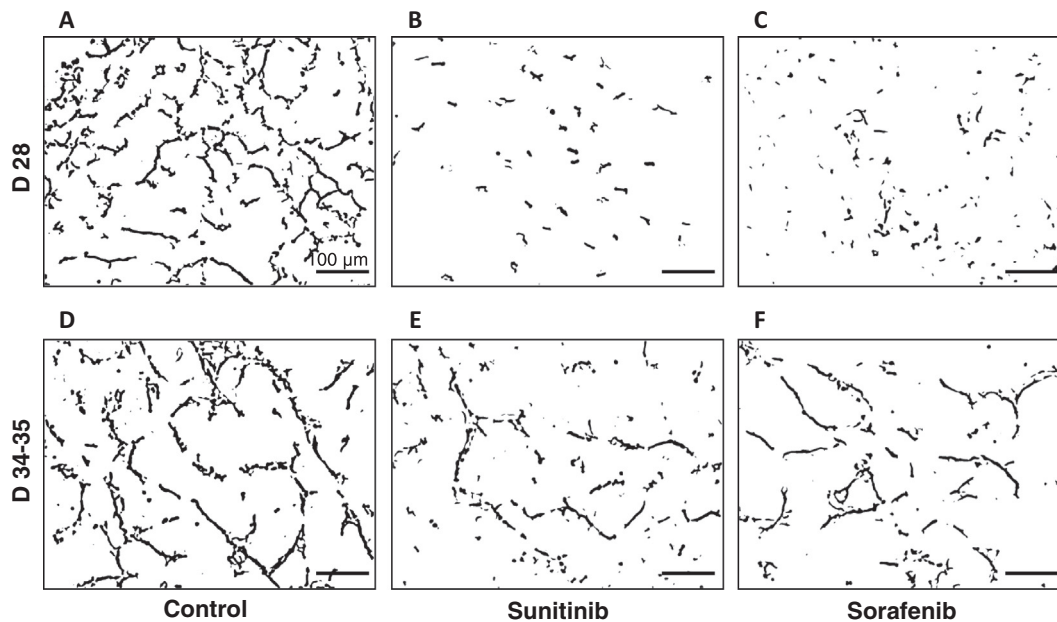

Fig. 3. Representative binarized images from microphotographs of control and treated tumor sections showing the vascular organization. CD31-immunohistochemical staining was performed after 14 days of treatment (D28) (A–C) and at the end of the experiment (D34/35) (D–F). Control tumors (A and D) displayed a dense vascular organization with linked segments of irregular length. Conversely, sunitinib- and sorafenib-treated tumors (B and C) showed a lower density of vascular entities with isolated labeled endothelial cells. One week after the treatment period (E and F), tumors exhibited more numerous and longer vessels than during the treatment (B and C). Magnification, 20×.

nodes. Therefore, both drugs were able to inhibit vessel sprouting leading to decreased tumor growth. These observations suggest that sunitinib and sorafenib most likely act on common targets such as VEGFR-2, a major effector of neo-angiogenesis, to inhibit blood vessel formation in pheochromocytoma. The effect of sunitinib on the microvascular density was comparable to that observed

in renal cell carcinoma xenografts [34]. However, treatment interruption provoked a rapid regrowth of tumor vessels, as has also been observed in lung carcinoma after withdrawal of a VEGF inhibitor [35], suggesting that a continuous treatment with these drugs is necessary to maintain the therapeutic effect. Such continuous treatment may provoke some toxic effects which should be
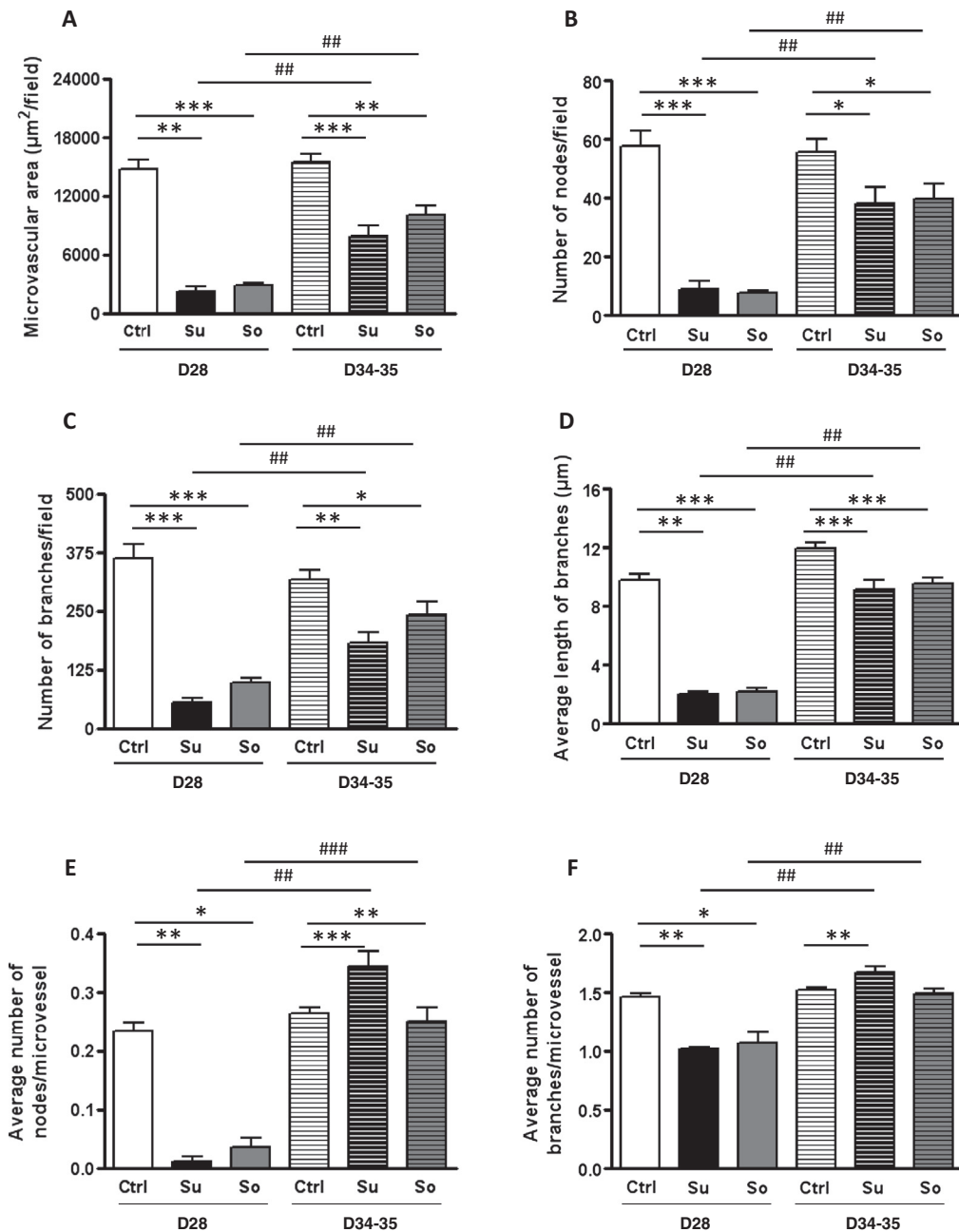
Fig. 4. Morphometric analysis of xenograft tumor vasculature. Quantitative analysis was performed from representative images as shown in Fig. 3. Values were calculated from control and sunitinib- or sorafenib-treated mice at both D28 and D34/35. The microvascular area (A), number of nodes (B) and branches (C) per field, length of microvessels (D) and the average number of nodes (E) and branches (F) per microvessel, were all significantly reduced by both treatments. *P < 0.05, **P < 0.01 and ***P < 0.001 for controls vs. treated comparisons; ##P < 0.01, ###P < 0.001 for D28-treated vs. D34/35-treated animals.

taken in consideration. We also observed a strong apoptosis after treatment with both drugs, although sunitinib seems to be a more potent effector of apoptosis than sorafenib *in vivo*. Other studies have reported that sunitinib and sorafenib could potently accelerate metastatic tumor growth after several weeks of treatment in xenograft-bearing mice [36–38]. Such a side effect was not observed in our model but additional studies using another PCC cell line with a malignant behavior, i.e. the MTT cell line [39] should be undertaken to test this possibility.

Besides their anti-angiogenic properties, we also demonstrated that both compounds had a direct effect on PC12 cells, in accordance with the expression of VEGFR-1, VEGFR-2, raf and RET in these cells [40–42]. Indeed, both sunitinib and sorafenib decreased cell viability within the nanomolar range, indicating that the VEGF signaling

pathway exerts a pro-tumoral effect in pheochromocytoma in an autocrine manner. As shown by their IC50, it appears that both drugs are more potent in PC12 cells (sunitinib IC50 = 0.07 μM; sorafenib IC50 = 0.02 μM) than in renal carcinoma cell lines (sunitinib IC50 ∼ 2–3 μM; sorafenib IC50 ∼ 0.3–3 μM) [24]. Interestingly, the efficient concentrations described here for PC12 cell growth inhibition (sunitinib IC50 ∼ 37 ng/mL and sorafenib IC50 ∼ 13 ng/mL) are lower than the mean plasma concentration (sunitinib 60–100 ng/mL [43] and sorafenib 5–7 μg/mL [44]) usually reported in treated patients, suggesting that the direct effects observed *in vitro* may also occur *in vivo* and would improve the efficacy of the drugs. The decrease in the number of cells could be ascribed to anti-proliferative and pro-apoptotic effects of these drugs. Thus, sunitinib could exert an anti-proliferative effect at low doses and
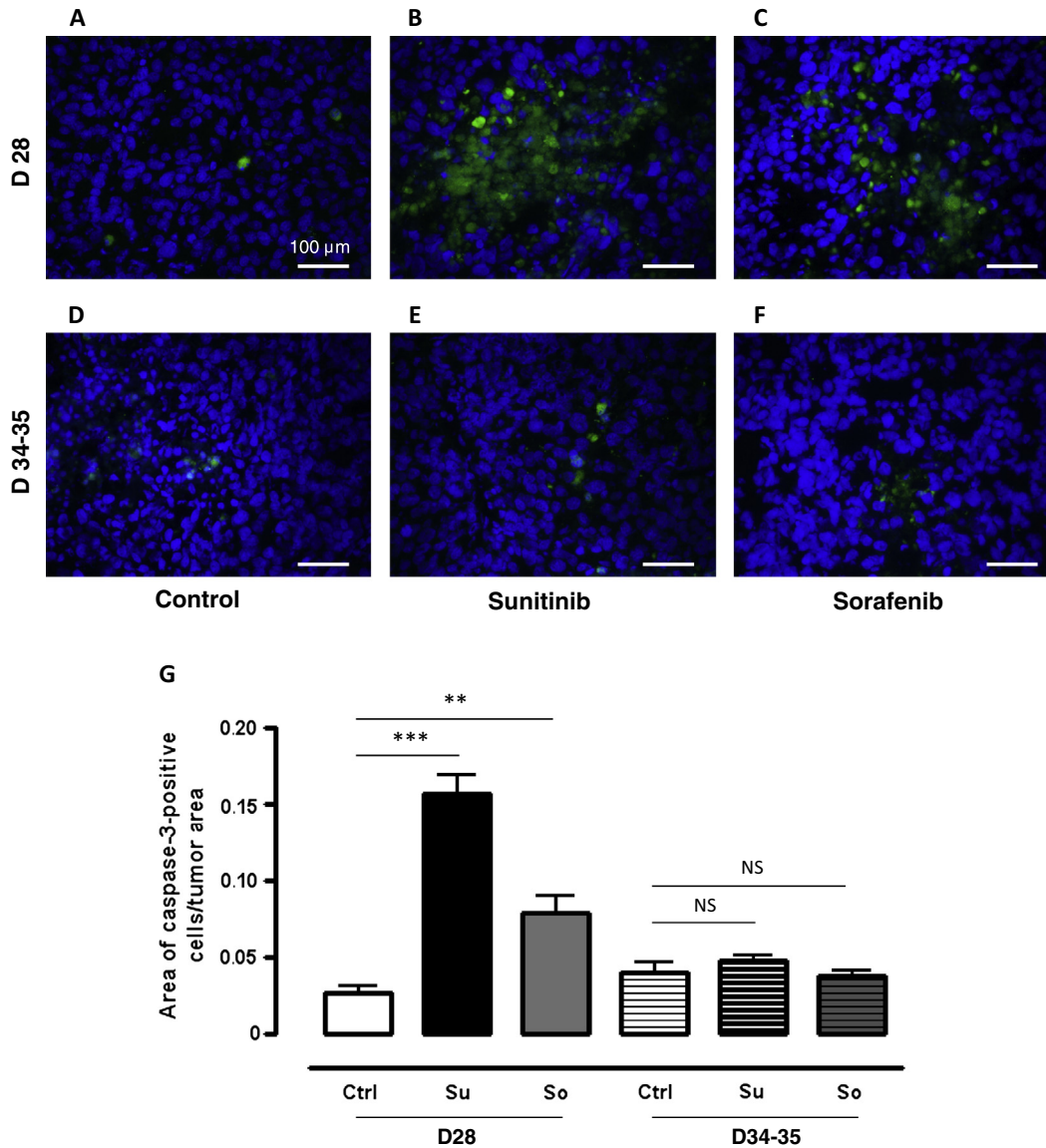
Fig. 5. Representative microphotographs of control (A and D) and sunitinib- or sorafenib-treated (B and E; C and F, respectively) tumors showing apoptotic cells (green color) at D28 and D34–35. Caspase-3 immunolabelling was quantified on entire tumor slices, and revealed that sunitinib and sorafenib significantly increased apoptosis after 14 days of treatment (D28) (G), whereas all tumors presented an equivalent level of apoptotic cells at D34–35. $^{**}P < 0.01$, $^{***}P < 0.001$, NS: not significant. *Blue*, dapi staining.

an apoptotic action at higher doses. In support of this hypothesis, we found that this drug exerted a potent pro-apoptotic effect at 30 μM but not at 3 or 10 μM, although the latter concentrations were effective in decreasing the number of cells. These observations are consistent with those of Saito et al. showing the pro-apoptotic effect of sunitinib in PC12 cells [42]. Whether the anti-proliferative effect of sunitinib in PC12 cells is also attributable to a down-regulation of the AKT/mTOR pathway following VEGFR-2 inhibition as has been shown for its pro-apoptotic action [42] remains to be established.

Although both drugs triggered tumoral cell death when administered *in vivo*, sorafenib, unlike sunitinib, did not exert any apoptotic effect *in vitro* as assessed by a caspase-3/7 activity test in PC12 cells after treatment. Interestingly, recent studies conducted on hepatocellular carcinoma or lymphoma cells also revealed a weak and inconstant apoptotic activity of sorafenib depending on the cell line [45,46]. It should be noted that sorafenib directly inhibits RAS/RAF/MAPK pathway which can incidentally activate the phosphorylation of AKT [47], leading to a compensatory cell survival mechanism. Nevertheless, sorafenib exerted a cytotoxic

effect in PC12 cells which could be ascribed to a caspase-3/7-independent cell death. It would be interesting to determine whether administration of PI3K/AKT inhibitors such as PI-103 could improve the inhibitory effect of sorafenib on pheochromocytoma tumor growth. If this were the case, sorafenib in combination with PI-103 would represent a better treatment than sorafenib or sunitinib alone, as synergistic or combinatorial effects of agents targeting several pathways are more likely to be effective in the long term [48].

In conclusion, our data obtained using a PCC model *in vivo*, provide strong pre-clinical evidence supporting the use of anti-angiogenic therapies in pheochromocytoma. We demonstrated a dual effect of both sunitinib and sorafenib to inhibit angiogenesis and tumoral cell survival in a pheochromocytoma xenograft model. While sunitinib efficacy has already been reported in a clinical study, our results indicate that sorafenib alone or in combination with other drugs targeting relevant pathways could also represent effective treatments for PCC. These treatments could be proposed at least for certain PCC subtypes characterized by heightened
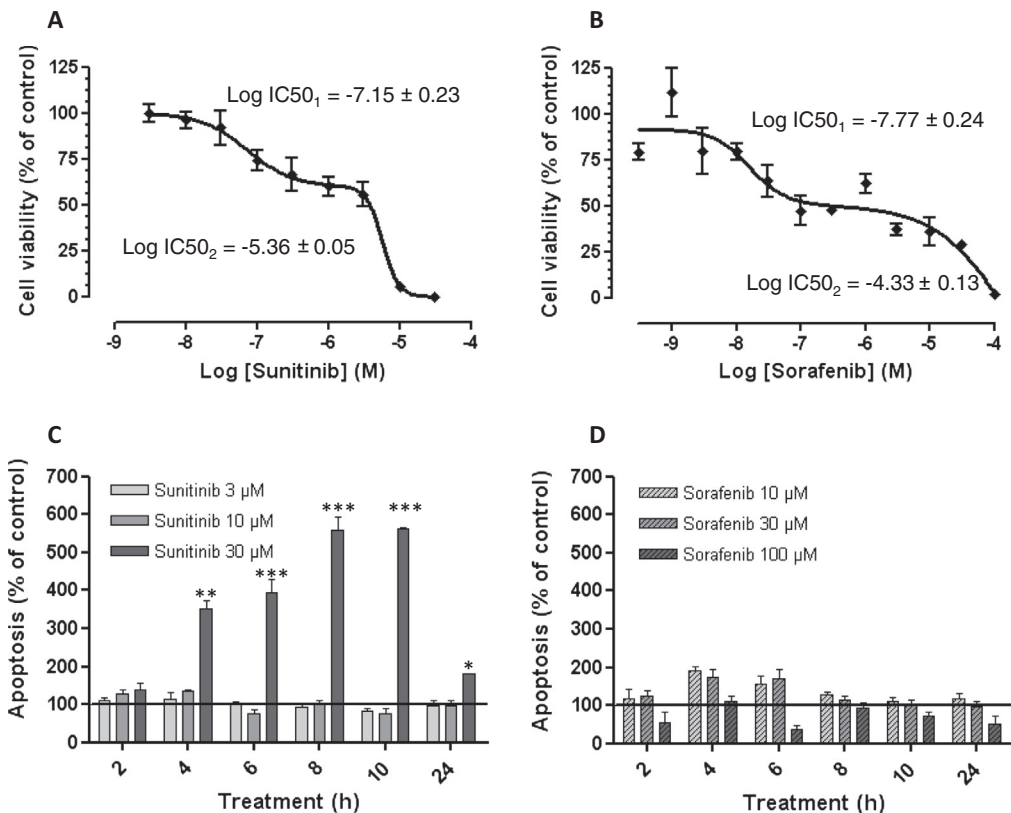
Fig. 6. Effect of sunitinib and sorafenib exposure on PC12 cells *in vitro*. Tumoral cells were cultured for 72 h in the presence of increased concentrations of sunitinib (A) and sorafenib (B), and cell viability was assessed. Both compounds induced anti-proliferative effects at low doses and cytotoxicity at high doses. Apoptosis was assessed from 2 to 24 h at doses ranging from 3 to 30 μM. Unlike sorafenib which was devoid of effect (D), sunitinib (30 μM) stimulated a massive and rapid increase of caspase-3/7-dependent PC12 cell apoptosis (C). $^{*}P < 0.05$, $^{**}P < 0.01$ and $^{***}P < 0.001$.

angiogenesis, such as malignant tumors and SDHx- and VHL-associated tumors in general.

Conflict of Interest

None declared.

Acknowledgments

References

[1] V. Kantorovich, K. Pacak, Pheochromocytoma and paraganglioma, Prog. Brain Res. 182 (2010) 343–373.
[2] L.J. Castro-Vega, A. Buffet, A.A. de Cubas, A. Cascón, M. Menara, E. Khalifa, L. Amar, S. Azriel, I. Bourdeau, O. Chabre, M. Curras-Freixes, V. Franco-Vidal, M. Guillaud-Bataille, C. Simian, A. Morin, R. Leton, A. Gomez-Grana, P.J. Pollard, P. Rustin, M. Robledo, J. Favier, A.P. Gimenez-Roqueplo, Germline mutations in FH confer predisposition to malignant pheochromocytomas and paragangliomas, Hum. Mol. Genet. (2013) 2440–2446.
[3] L. Fishbein, K.L. Nathanson, Pheochromocytoma and paraganglioma: understanding the complexities of the genetic background, Cancer Genet. 205 (2012) 1–11.
[4] J. Favier, A.P. Gimenez-Roqueplo, Pheochromocytomas: the (pseudo)-hypoxia hypothesis, Best Pract. Res. Clin. Endocrinol. Metab. 24 (2010) 957–968.
[5] S. Nölting, A.B. Grossman, Signaling pathways in pheochromocytomas and paragangliomas: prospects for future therapies, Endocr. Pathol. 23 (2012) 21–33.
[6] C. Jimenez, E. Rohren, M.A. Habra, T. Rich, P. Jimenez, M. Ayala-Ramirez, E. Baudin, Current and future treatments for malignant pheochromocytoma and sympathetic paraganglioma, Curr. Oncol. Rep. 15 (2013) 356–371.
[7] L. Amar, Genetic testing in pheochromocytoma or functional paraganglioma, J. Clin. Oncol. 23 (2005) 8812–8818.
[8] M. Ayala-Ramirez, L. Feng, M.M. Johnson, S. Ejaz, M.A. Habra, T. Rich, N. Busaidy, G.J. Cote, N. Perrier, A. Phan, S. Pate, S. Waquespack, C. Jimenez, Clinical risk factors for malignancy and overall survival in patients with pheochromocytomas and sympathetic paragangliomas: primary tumor size and primary tumor location as prognostic indicators, J. Clin. Endocrinol. Metab. 96 (2011) 717–725.
[9] J. Favier, P.F. Plouin, P. Corvol, J.M. Gasc, Angiogenesis and vascular architecture in pheochromocytomas: distinctive traits in malignant tumors, Am. J. Pathol. 161 (2002) 1235–1246.
[10] K. Salmenkivi, P. Heikkilä, J. Liu, C.A.J. Haglund, J. Arola, VEGF in 105 pheochromocytomas: enhanced expression correlates with malignant outcome, APMIS 111 (2008) 458–464.
[11] A. Zielke, M. Middeke, S. Hoffmann, M. Colombo-Benkmann, P. Barth, I. Hassan, A. Wunderlich, C. Lorenz, Q.Y. Duh, EGF-mediated angiogenesis of human pheochromocytomas is associated to malignancy and inhibited by anti-VEGF antibodies in experimental tumors, Surgery 132 (2002) 1056–1063.
[12] J. Favier, P. Igaz, N. Burnichon, L. Amar, R. Libé, C. Badoual, F. Tissier, J. Bertherat, P.F. Plouin, X. Jeunemaitre, A.P. Gimenez-Roqueplo, Rationale for anti-angiogenic therapy in pheochromocytoma and paraganglioma, Endocr. Pathol. 23 (2011) 34–42.
[13] Q. Liu, G. Djuricin, E.D. Staren, P. Gattuso, V.E. Gould, J. Shen, T. Saclarides, D.B. Rubin, R.A. Prinz, Tumor angiogenesis in pheochromocytomas and paragangliomas, Surgery 120 (1996) 938–942.
[14] P.P. Rooijens, R.R. de Krijger, H.J. Bonjer, F. van der Ham, A.L. Nigg, H.A. Bruining, S.W. Lamberts, E. Harst, The significance of angiogenesis in malignant pheochromocytomas, Endocr. Pathol. 15 (2004) 39–45.
[15] K.J. Gotink, H.M.W. Verheul, Anti-angiogenic tyrosine kinase inhibitors: what is their mechanism of action?, Angiogenesis 13 (2009) 1–14
[16] N.M. Hahn, M. Reckova, L. Cheng, L.A. Baldridge, O.W. Cummings, C.J. Sweeney, Patient with malignant paraganglioma responding to the multikinase inhibitor sunitinib malate, J. Clin. Oncol. 27 (2009) 460–463.
[17] C. Jimenez, M.E. Cabanillas, L. Santarpia, E. Jonasch, K.L. Kyle, E.A. Lano, S.F. Matin, R.F. Nunez, N.D. Perrier, A. Phan, T.A. Rich, B. Shah, M.D. Williams, S.G. Waguespack, Use of the tyrosine kinase inhibitor sunitinib in a patient with von Hippel–Lindau disease: targeting angiogenic factors in pheochromocytoma

and other von Hippel–Lindau disease-related tumors, J. Clin. Endocrinol. Metab. 94 (2009) 386–391.

[18] A.M. Joshua, S. Ezzat, S.L. Asa, A. Evans, R. Broom, M. Freeman, J.J. Knox, Rationale and evidence for sunitinib in the treatment of malignant paraganglioma/pheochromocytoma, J. Clin. Endocrinol. Metab. 94 (2009) 5–9.

[19] F. Sun, H. He, T. Su, W. Zhou, X. Huang, J. Dai, Z.J. Shen, Multi-targeted tyrosine kinase inhibitor sunitinib: a novel strategy for sporadic malignant pheochromocytoma, Chin. Med. J. 125 (2012) 2231–2234.

[20] K.S. Park, J.L. Lee, H. Ahn, J.M. Koh, I. Park, J.S. Choi, Y.R. Kim, T.S. Park, J.H. Ahn, D.H. Lee, T.W. Kim, J.S. Lee, Sunitinib, a novel therapy for anthracycline- and cisplatin-refractory malignant pheochromocytoma, Jpn. J. Clin. Oncol. 39 (2009) 327–331.

[21] M. Ayala-Ramirez, C.N. Chougnet, M.A. Habra, J.L. Palmer, S. Leboulleux, M.E. Cabanillas, C. Caramella, P. Anderson, A. Al Ghuzlan, S.G. Waguespack, D. Deandreis, E. Baudin, C. Jimenez, Treatment with sunitinib for patients with progressive metastatic pheochromocytomas and sympathetic paragangliomas, J. Clin. Endocrinol. Metab. 97 (2012) 4040–4050.

[22] D.B. Mendel, A.D. Laird, X. Xin, S.G. Louie, J.G. Christensen, G. Li, R.E. Schreck, T.J. Abrams, T.J. Ngai, L.B. Lee, L.J. Murray, J. Carver, E. Chan, K.G. Moss, J.O. Haznedar, J. Sukbuntherng, R.A. Blake, L. Sun, C. Tang, T. Miller, S. Shirazian, G. McMahon, J.M. Cherrington, In vivo antitumor activity of SU11248, a novel tyrosine kinase inhibitor targeting vascular endothelial growth factor and platelet-derived growth factor receptors determination of a pharmacokinetic/ pharmacodynamic relationship, Clin. Cancer Res. 9 (2003) 561–574.

[23] Y.S. Chang, J. Adnane, P.A. Trail, J. Levy, A. Henderson, D. Xue, E. Bortolon, M. Ichetovkin, C. Chen, A. McNabola, D. Wilkie, C.A. Carter, I.C. Taylor, M. Lynch, S. Wilhelm, Sorafenib (BAY 43-9006) inhibits tumor growth and vascularization and induces tumor apoptosis and hypoxia in RCC xenograft models, Cancer Chemother. Pharmacol. 59 (2007) 561–574.

[24] M. Miyake, S. Anai, K. Fujimoto, S. Ohnishi, M. Kuwada, Y. Nakai, T. Inoue, A. Tomioka, N. Tanaka, Y. Hirao, 5-Fluorouracil enhances the antitumor effect of sorafenib and sunitinib in a xenograft model of human renal cell carcinoma, Oncol. Lett. 3 (2012) 1195–1202.

[25] J. Schindelin, I. Arganda-Carreras, E. Frise, V. Kaynig, M. Longair, T. Pietzsch, S. Preibisch, C. Rueden, S. Saalfeld, B. Schmid, J.Y. Tivenez, D.J. White, V. Hartenstein, K. Eliceiri, P. Tomancak, A. Cardona, Fiji: an open-source platform for biological-image analysis, Nat. Meth. 9 (2012) 676–682.

[26] K.E. Oberg, O. Casanovas, J.P. Castano, D.C. Chung, G. Delle Fave, P. Denefle, P. Harris, M.S. Khan, M.H. Kulke, A. Scarpa, L.H. Tang, B. Wiedenmann, Molecular pathogenesis of neuroendocrine tumors: implications for current and future therapeutic approaches, Clin. Cancer Res. 19 (2013) 2842–2849.

[27] G. Parenti, B. Zampetti, E. Rapizzi, T. Ercolino, V. Giachè, M. Mannelli, Updated and new perspectives on diagnosis, prognosis, and therapy of malignant pheochromocytoma/paraganglioma, J. Oncol. 2012 (2012) 1–10.

[28] S. Nölting, A. Giubellino, Y. Tayem, K. Young, M. Lauseker, P. Bullova, J. Schovanek, M. Anver, S. Fliedner, M. Korbonits, B. Göke, G. Vlotibes, A. Grossman, K. Pacak, Combination of 13-cis retinoic acid and lovastatin: marked antitumor potential in vivo in a pheochromocytoma allograft model in female athymic nude mice, Endocrinology 155 (2014) 2377–2390.

[29] M.E. Bourcier, A.I. Vinik, Sunitinib for the treatment of metastatic paraganglioma and vasoactive intestinal polypeptide-producing tumor (VIPoma), Pancreas 42 (2013) 348–352.

[30] T. Prochilo, G. Savelli, P. Bertocchi, C. Abeni, L. Rota, A. Rizzi, A. Zaniboni, Targeting VEGF-VEGFR pathway by sunitinib in peripheral primitive neuroectodermal tumor, paraganglioma and epithelioid hemangioendothelioma: three case reports, Case Rep. Oncol. 6 (2013) 90–97.

[31] M.H. Kulke, J. Bendell, L. Kvols, J. Picus, R. Pommier, J. Yao, Evolving diagnostic and treatment strategies for pancreatic neuroendocrine tumors, J. Hematol. Oncol. 4 (2011) 29.

[32] A. Zielke, R.S. Bresalier, A.E. Siperstein, O.H. Clark, M. Rothmund, Q.Y. Duh, A unique allogenic model of metastatic pheochromocytoma: PC12 rat pheochromocytoma xenografts to nude mice and establishment of metastases-derived PC12 variants, Clin. Exp. Metast. 16 (1998) 341–352.

[33] Y. Maitani, H. Saito, Y. Seishi, Y. Iwase, T. Yamauchi, K. Higashiyama, T. Sugino, A combination of liposomal sunitinib plus liposomal irinotecan and liposome

[34] D. Huang, Y. Ding, Y. Li, W.M. Luo, Z.F. Zhang, J. Snider, K. Vandenbeldt, C.N. Qian, B.T. Teh, Sunitinib acts primarily on tumor endothelium rather than tumor cells to inhibit the growth of renal cell carcinoma, Cancer Res. 70 (2010) 1053–1062.

[35] M.R. Mancuso, R. Davis, S.M. Norberg, S. O'Brien, B. Sennino, T. Nakahara, V.J. Yao, T. Inai, P. Brooks, B. Freimark, D.R. Shalinsky, D.D. Hu-Lowe, D.M. McDonald, Rapid vascular regrowth in tumors after reversal of VEGF inhibition, J. Clin. Invest. 116 (2006) 2610–2621.

[36] J.M.L. Ebos, C.R. Lee, R.S. Kerbel, Tumor and host-mediated pathways of resistance and disease progression in response to antiangiogenic therapy, Clin. Cancer Res. 15 (2009) 5020–5025.

[37] M. Pàez-Ribes, E. Allen, J. Hudock, T. Takeda, H. Okuyama, F. Viñals, M. Inoue, G. Bergers, D. Hanahan, O. Casanovas, Antiangiogenic therapy elicits malignant progression of tumors to increased local invasion and distant metastasis, Cancer Cell 15 (2009) 220–231.

[38] W. Zhang, H. Sun, W. Wang, Q. Zhang, P. Zhuang, Y. Xiong, Sorafenib down-regulates expression of HTATIP2 to promote invasiveness and metastasis of orthotopic hepatocellular carcinoma tumors in mice, Gastroenterology 143 (2012) 1641–1649.

[39] L. Martiniova, E.W. Lai, A.G. Elkahloun, M. Abu-Asab, A. Wickremasinghe, D.C. Solis, S.M. Perera, T.T. Huynh, I.A. Lubensky, A.S. Tischler, R. Kvetnansky, S. Alesci, J.C. Morris, K. Pacak, Characterization of an animal model of aggressive metastatic pheochromocytoma linked to a specific gene signature, Clin. Exp. Metast. 26 (2009) 239–250.

[40] G.D. Vita, R.M. Melillo, F. Carlomagno, R. Visconti, M.D. Castellone, A. Bellacosa, M. Billaud, A. Fusco, P.N. Tsichlis, M. Santoro, Tyrosine 1062 of RET-MEN2A mediates activation of Akt (Protein Kinase B) and mitogen-activated protein kinase pathways leading to PC12 cell survival, Cancer Res. 60 (2000) 3727–3731.

[41] P. Peraldi, M. Frödin, J.V. Barnier, V. Calleja, J.C. Scimeca, C. Filloux, G. Calothy, E. Van Obberghen, Regulation of the MAP kinase cascade in PC12 cells: B-raf activates MEK-1 (MAP kinase or ERK kinase) and is inhibited by cAMP, FEBS Lett. 357 (1995) 290–296.

[42] Y. Saito, Y. Tanaka, Y. Aita, K. Ishii, T. Ikeda, K. Isobe, Y. Kawakami, H. Shimano, H. Hara, K. Takekoshi, Sunitinib induces apoptosis in pheochromocytoma tumor cells by inhibiting VEGFR2/Akt/mTOR/S6K1 pathways through modulation of Bcl-2 and BAD, Am. J. Physiol. Endocrinol. Metab. 302 (2012) 615–625.

[43] N.A. Lankheet, L.M. Knapen, J.H. Schellens, J.H. Beijnen, N. Steeghs, A.D. Huitema, Plasma concentrations of tyrosine kinase inhibitors imatinib, erlotinib, and sunitinib in routine clinical outpatient cancer care, Ther. Drug Monit. 36 (2013) 326–334.

[44] D. Strumberg, H. Richly, R.A. Hilger, N. Schleucher, S. Korfee, M. Tewes, M. Faghih, E. Brendel, D. Voliotis, C.G. Haase, B. Schwartz, A. Awada, R. Voigtmann, M.E. Scheulen, S. Seeber, Phase I clinical and pharmacokinetic study of the novel raf kinase and vascular endothelial growth factor receptor inhibitor BAY 43-9006 in patients with advanced refractory solid tumors, J. Clin. Oncol. 23 (2005) 965–972.

[45] A. Galmiche, B. Chauffert, J.-C. Barbare, New biological perspectives for the improvement of the efficacy of sorafenib in hepatocellular carcinoma, Cancer Lett. 346 (2013) 159–162.

[46] C. Carlo-Stella, S.L. Locatelli, A. Giacomini, L. Cleris, E. Saba, M. Righi, A. Guidetti, A.M. Gianni, Sorafenib inhibits lymphoma xenografts by targeting MAPK/ERK and AKT pathways in tumor and vascular cells, PLoS ONE 8 (2013) e61603.

[47] R. Gedaly, P. Angulo, C. Chen, K.T. Creasy, B.T. Spear, J. Hundley, M.F. Daily, M. Shah, B.M. Evers, The role of PI3K/mTOR inhibition in combination with sorafenib in hepatocellular carcinoma treatment, Anticancer Res. 32 (2012) 2531–2536.

[48] S. Nölting, E. Garcia, G. Alusi, A. Giubellino, K. Pacak, M. Korbonits, A.B. Grossman, Combined blockade of signalling pathways shows marked anti-tumour potential in phaeochromocytoma cell lines, J. Mol. Endocrinol. 49 (2012) 79–96.